Military Technical College, Kobry El-Kobbah, Cairo, Egypt

9th International Conference On Aerospace Sciences & Aviation Technology

THEORETICAL AND EXPERIMENTAL STUDY ON PERFORMANCE OF VARIABLE SPEED TRACTION DRIVES

YOUNES* Y.K, EL-DANNANAH ** E.H., MANSOUR*** H.A.H. and MAHMOUD**** M.F.Y.

ABSTRACT

The paper deals with a theoretical and experimental evaluation of variable speed traction drive performance characteristics.These include their torque capacity, power rating, efficiency of transmission and percentage slip. Drives with a single and double counterformal Hertzian contacts have been analyzed to derive non-dimensional design expressions. Constant traction coefficient pertinent to the boundary lubrication mode nearing thin fluid film friction is adopted to evaluate torque and power ratings. An actual test rig with a single traction contact has been designed and used to get experimental values of the traction capacity and efficiency of power transmission in the range below the limits of gross slippage. Comparison between theory and experiments shows good correlation and promises for high efficiency of transmission and power to volume ratios.

KEY WORDS

Traction drives, Stepless speed reduction, Power transmission, Rolling, Spinning, Hertzian contacts.

Professor, ** Associate Professor, *** Assistant Professor, **** Assistant Lecturer
Mechanical design dpt., Faculty of Engineering-Mataria, Helwan University, Cairo

INTRODUCTION

To date, traction drives are still considered attractive power transmission systems for modern industrial applications where continuous (stepless) speed regulation is required. For nearly a century a variety of patents appeared and have been efficiently used in automotive, textile and machine tool industries, [1-2-3]. In these drives power is transmitted through traction forces generated in the Hertzian contact areas of the loaded rolling elements, [4-5]. Although the principle of operation is common, each drive has its own design and construction features, power to weight ratio, transmission ratio ranges and efficiency ratings. Design guides or equations are not extensively available for these drives. Most manufacturers report their own drive characteristics, usually obtained from actual product testing. This does not provide a design scheme for the designer to proceed in the design process for specific duty requests. In addition, most of the research work concentrates on specific drive designs,[6-7]. This does not lead to a generalized classification and a base for performance comparisons in terms of torque capacity, slip, efficiency of transmission and power to size or weight ratios.

THEORY

The basic idea of traction drives is illustrated in Fig.1. Power is transmitted from one element to the other through the combined roll-slide action within a common Hertzian contact area, enlarged under the normal component of the applied compressive load. The sum of moments of the differential tractive forces, around the axes of rotation give the torques on the driving and resisting shafts. For a specific torque demand on the driven element shaft, a corresponding spin point will be located a distance m from the center of contact. At this point the relative sliding velocity is zero. In the case of a double contact drive (with an intermediate element) two spin points exist. Their locations are specified from the torque equilibrium of the intermediate element i.e.:

Torque from the driving element = Torque applied from the resisting element

In this case, the transmission ratio at loaded conditions (m m′ 0) will be:

$$T_r = \frac{\omega_{out}}{\omega_{in}} = \frac{s}{s_1} = \frac{R-m}{R'+m'} \tag{1}$$

where R and R are the contact radii of both the driving and the driven disks with the intermediate one. Accordingly the percentage slip when the drive is loaded is:

$$S\% = 1 - \frac{R-m}{R'+m'}\left(\frac{R'}{R}\right) x100\% \tag{2}$$

At any point within the contact surfaces a differential tractive force dF will act in the direction of the sliding velocity Vs. Thus, the torque transmitted from one element to the other will be;

$$T = \iint d\bar{F}r = \mu \iint \sigma r dA \tag{3}$$

Where σ is the Hertzian compressive stress and μ is the traction coefficient.
Due to the geometric slippage over the contacting surfaces, the power lost per contact can be evaluated after performing the following integral:

$$\text{Power Lost} = \quad V_s \,.\, dF \tag{4}$$

Consequently, the efficiency of power transmission will be:

$$\% = [(\text{Input power} - \text{Power loss}) / (\text{Input power})] \times 100 \tag{5}$$

For a general elliptical contact area the above-defined integrations are elaborate because the differential traction forces have different directions in the plane of the contact surfaces. In addition, the Hertzian stress distribution has an ellipsoidal form over the contact.
Defining the following non dimensional parameters:

Aspect ratio of the contact area $K_1 = b / a$ (6)

Aspect ratio of the drive $K = b / r$ (7)

Center point location parameter $K_2 = Rc / b$ (8)

Spin point location parameter $K_3 = m / b$ (9)

Stress parameter
$$P_1 = \frac{\sigma}{\sigma_{max}} = \sqrt{1 - X^2 - Y^2} \tag{10}$$

Sliding velocity parameter
$$P_2 = \frac{V_s}{\omega_1 b} = \sqrt{(K_3 + Y^2) + (X/K_1)^2} \tag{11}$$

Torque arm parameter
$$P_3 = (K_2 + Y)(K_3 + Y) + \left(\frac{X}{K_1}\right)^2 \tag{12}$$

Where $X = x/a$ and $Y = y/b$, (a and b are the semi major axes of the contact)

After proper substitutions, the different drive performance characteristics can be evaluated. The double integrals will then be performed over the area of a circle, which is the transformation of the elliptical contact. Tables 1 and 2 summarize the expressions used for evaluating performance merits at selected geometrical and running conditions.

TEST RIG DESCRIPTION

Referring to Figs 3 and 4, an overview of the designed test rig and its constructional details are presented. The drive consists of two rolling disks with a rim to face arrangement. The driving disk is the large one, (= 240mm). It is made of steel with lapped surface and rotates with the constant speed of the motor =1500 rpm. It can slide axially along its shaft via a spline. This construction allows a continuous application of the contact force against the driven disk. The later consists of two steel disks clamping a hollow cylindrical wheel made of Asbestos having a modulus of elasticity value=2500 Mpa. Speed regulation is achieved by rotating a screw through a knob to adjust the transmission ratio at a desired value.

Table 1 performance characteristics of the point contact drives

	Parametric form	Nondimensional form
Transmission ratio	$\frac{R_c - m}{r}$	$K(K_2 - K_3)$
input torque	$\mu \sigma_m b^2 a \iint \frac{P_1 P_3}{P_2} dXdY$	$\bar{T}_i = \frac{T_i}{\mu \sigma_m b r^2} = \frac{K^2}{K_1} \iint \frac{P_1 P_3}{P_2} dXdY$
Input power	$\mu \sigma_m b^2 a \omega_1 \iint \frac{P_1 P_3}{P_2} dX\, dY$	$\bar{P}_i = \frac{P_i}{\mu \sigma_m b r^2 \omega_1} = \frac{K^2}{K_1} \iint \frac{P_1 P_3}{P_2} dXdY$
Power loss	$\mu \sigma_m b^2 a \omega_1 \iint P_1 P_2 dXdY$	$\bar{P}_L = \frac{P_L}{\mu \sigma_m b r^2 \omega_1} = \frac{K^2}{K_1} \iint P_1 P_2 dXdY$
Output power	$\mu \sigma_m b^2 a \omega_1 \iint \left[\iint \frac{P_1 P_3}{P_2} dXdY - \iint P_1 P_2 dXdY \right]$	$\bar{P}_o = \frac{P_o}{\mu \sigma_m b r^2 \omega_1} = \frac{K^2}{K_1} \iint \left[\iint \frac{P_1 P_3}{P_2} dXdY - \iint P_1 P_2 dXdY \right]$
Output torque	$\frac{\mu \sigma_m b^2 a}{T_r} \left[\iint \frac{P_1 P_3}{P_2} dXdY - \iint P_1 P_2 dXdY \right]$	$\bar{T}_o = \frac{T_o}{\mu \sigma_m b r^2} = \frac{K^2}{K_1 T_r} \left[\iint \frac{P_1 P_3}{P_2} dXdY - \iint P_1 P_2 dXdY \right]$
Efficiency	$\eta)_{23} = 1 - \frac{\iint P_1 P_2 dXdY}{\iint \frac{P_1 P_3}{P_2} dXdY}$	$\eta)_{23} = 1 - \frac{\iint P_1 P_2 dXdY}{\iint \frac{P_1 P_3}{P_2} dXdY}$

Table 2 Performance characteristics of double points contact drives

	Parametric form	Nondimensional form
Transmission ratio	$\frac{R_c - m}{R_c' + m'}$	$\frac{K_2 - K_3}{K_2' + K_3'}$
Input torque	$\mu \sigma_m b^2 a T_r)_{12} \left[\iint \frac{P_1 P_3'}{P_2'} dXdY - \iint P_1 P_2' dXdY \right]$	$\bar{T}_i = \frac{T_i}{\mu \sigma_m b r^2} = \frac{K^2 T_r)_{12}}{K_1} \left[\iint \frac{P_1 P_3'}{P_2'} dXdY - \iint P_1 P_2' dXdY \right]$
Input power	$\mu \sigma_m b^2 a \omega_2 \left[\iint \frac{P_1 P_3'}{P_2'} dXdY + \iint P_1 P_2' dXdY \right]$	$\bar{P}_i = \frac{P_i}{\mu \sigma_m b r^2 \omega_1} = \frac{K^2 T_r)_{12}}{K_1} \left[\iint \frac{P_1 P_3'}{P_2'} dXdY + \iint P_1 P_2' dXdY \right]$
Output torque	$\frac{\mu \sigma_m b^2 a}{T_r)_{23}} \left[\iint \frac{P_1 P_3}{P_2} dXdY - \iint P_1 P_2 dXdY \right]$	$\bar{T}_o = \frac{T_o}{\mu \sigma_m b r^2} = \frac{K^2}{K_1 T_r)_{23}} \left[\iint \frac{P_1 P_3}{P_2} dXdY - \iint P_1 P_2 dXdY \right]$
Output power	$\mu \sigma_m b^2 a \omega_2 \left[\iint \frac{P_1 P_3}{P_2} dXdY - \iint P_1 P_2 dXdY \right]$	$\bar{P}_o = \frac{P_o}{\mu \sigma_m b r^2 \omega_1} = \frac{K^2 T_r)_{12}}{K_1} \left[\iint \frac{P_1 P_3}{P_2} dXdY - \iint P_1 P_2 dXdY \right]$
Power loss	$\mu \sigma_m b^2 a \omega_2 \left[\iint P_1 P_2 dXdY + \iint P_1 P_2' dXdY \right]$	$\bar{P}_L = \frac{P_L}{\mu \sigma_m b r^2 \omega_1} = \frac{K^2 T_r)_{12}}{K_1} \left[\iint P_1 P_2 dXdY + \iint P_1 P_2' dXdY \right]$
Efficiency	$\frac{\iint (P_1 P_3 \; P_2) dXdY - \iint P_1 P_2 dXdY}{\iint \left(P_1 P_3' \; P_2' \right) dXdY + \iint P_1 P_2' dXdY}$	

The driven wheel is displaced axially by means of a fork engaged to the wheel by two side supports. The output shaft can have zero rotational speed when the contact point lies on the driving shaft axis. Reversed rotational speeds can be obtained by positioning the driven wheel at both sides of the axis of the driving wheel along its traction face. Thus, the drive with this design is an Infinitely Variable Transmission (IVT). A two-arm lever with a central seat can apply the compressive load. Two steel wires pull the two arms under the action of a dead weight. A cup and cone
braking system provides the application of the resisting torque. Torsional resisting moment is measured by means of a four-strain gage arrangement. Proper calibration has been conducted for the system before acquiring the test results.

DISCUSSION OF RESUTS

A computer program has been developed to perform the different integrals shown in Tables 1 and 2 in order to evaluate the performance characteristics of the rim to face drive. Single and double contact configurations were considered in the study,[8]. Figs.5 and 6 show the variation of the relative slip and efficiency of power transmission versus the applied resisting torque for different transmission ratios. The relative slip varies linearly with the load and then it increases sharply where maximum traction capacity of the contact is reached. The spin at high loads is located far away from the center of the contact and the differential tractive forces align themselves in a parallel direction. In addition, the relative sliding speeds increase in magnitude and which lead to an increase in the power lost as shown in Fig.6. In practice gross slip may occur at high levels of applied resisting torque where contacts lose grip and efficiencies drop drastically. Referring to Figs.7 and 8, the increase of the normal compressive force while maintaining a constant value for the traction coefficient (0.2), has two main effects. The first is the increase of the Hertzian contact stresses and the second is the enlargement of the contact area. These will lead to a higher torque capacity but with an increase of the relative slip and consequently a drop in the power transmission efficiency is expected.
The change in the contact conformity r''/r will change the ellipticity parameter b/a. A long elliptical contact oriented along the tangential direction will provide better efficiencies a shown in Fig.9. An elliptical contact with its long axis oriented along the radial direction will provide higher torque capacity but local sliding speeds will increase leading to lower efficiencies. This is due to the relative position of the spin point with respect to the contact center at different applied torque levels. Fig.10, shows the amount of power lost when the drive operates with two rolling disks and an intermediate one. Losses in each contact will depend on the relative position of each spin point. As shown in Fig.11, the overall efficiency drops when compared to the single contact drive under the same Hertzian loads and conformity.
Referring to Figs.12 and 13, the output speed was measured experimentally at different levels of resisting torque in order to evaluate the amount of slip ,i.e the variation of the output speed from the expected nominal value calculated from the wheel radii ratio. Actually, under different running conditions, the traction coefficient value may decrease from the value evaluated at the calibration condition. To estimate the performance characteristics in the theoretical analyses the traction coefficient is maintained constant.
Figs.14 and 15 show the effect of increasing the width of the driven rolling element,(the line contact case). Longer contact areas have higher losses as

discussed before. Thus relative slip is higher and consequently the output speed will relatively decrease for the same compressive load (90 N), transmission ratio and applied resisting torque. The effect of contact area location with respect to the driving disk center on the power transmission efficiency is shown in Fig.16. At high transmission ratios spinning action is more pronounced in magnitude. This situation tends to increase losses due to the geometrical slippage which exists even at no load conditions.

CONCLUSIONS

Several conclusions may be reported from the work presented in this paper and which may help traction drive designers to achieve high performance for a power transmission demand.
Despite of their wide range of transmission ratio, the double contact drives show lower efficiencies than the drives with a single contact. In addition, contact areas should be as small as possible by proper use of rolling element radii combinations.
An increase in the geometric slippage losses in expected when the working compressive stresses are increased. This is due to the enlargement of the contact areas and consequently the of the relative sliding velocities, especially at high resisting torque demands where the spin point is far from the contact centers.
The torque capacity of a drive is controlled by several criteria. The first is the increase of the compressive stresses but to the surface endurance limits. The second by designing the rolling elements with large dimensions, but to the limit where the power to weight ratio is not acceptable. The third is the gross slippage where the rolling sliding elements loose grip and traction effectiveness fails. The fourth is the increase of traction coefficient. This factor is limited when lubricants are used to prevent wear and excessive heat generation.
The non-dimensional performance terms reported in this study help the theoretical analyses of new drive designs as a prerequisite for prototype testing.

REFERENCES

[1] Edson,D.V. ' Continuously Variable Transmission :a Concept whose Time has come', Design News / 1-5-81 p.55, (1981)
[2] George Sauer, ' Continuously Variable Transmission for Tractor Drive Line', Institute of Agricultural Machinery, Technical University of Munich, Germany /May, (1996)
[3] Kevin Clemens, 'Technology of the Year 1996 Honda's Continuously Variable Transmission', Automobile Magazine, January, (1996)
[4] Younes,Y.K., 'A Design Scheme for Multi-Disk Beier Traction Variators' ASME Trans, Journal of Mechanical Design'Vol.114,pp 17-22,(1992)
[5] Lingard,S., 'Tractions at the Spinning Point Contacts of a Variable Ratio Friction Drive',Tribology International,p 228,October, (1974)
[6] Hisashi,M. and Nobuhide,K., 'Prototype Design and Testing of the Half Toroidal CVT', SAE Technical Papers Series No.900552, (1990)
[7] Imanishi,T. and Machida,H., 'A Geometric Study of Toroidal CVT – A Comparison of Half-Toroidals and Full-Toroidals', ASE, (1996)
[8] Mahmoud M.F.Y.,' A Study of Optimal Power Ratings For Variable Speed Traction Drives', MSc Thesis, Mechanical Design Dpt, Faculty of Eng. Helwan University,(2000)

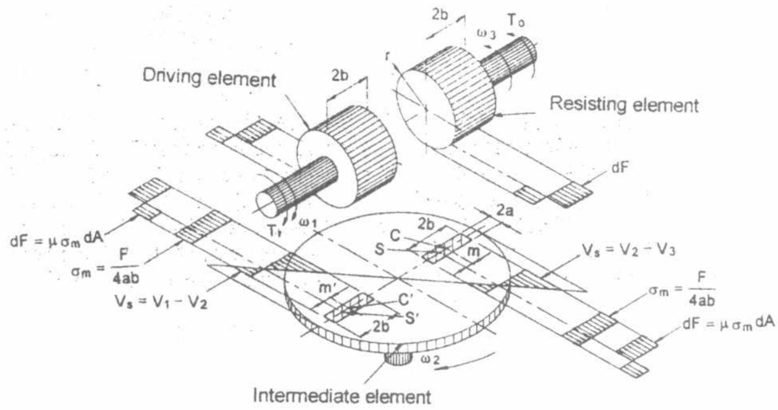

Fig.1. General geometrical and kinematical relations of a double line contact drive

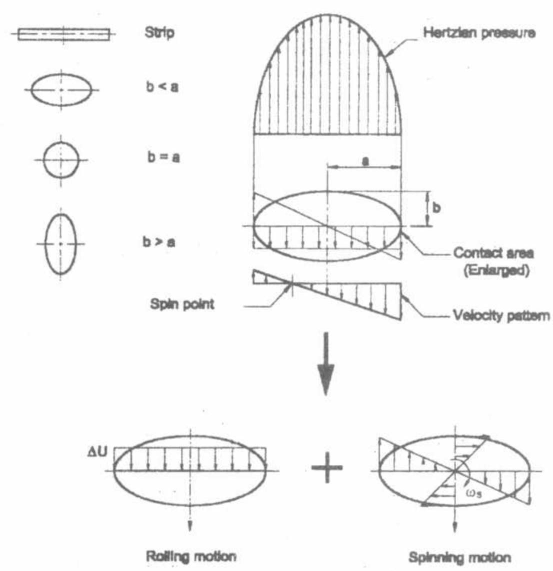

Fig.2. Hertzian contact area with various velocities as occurring in traction drive

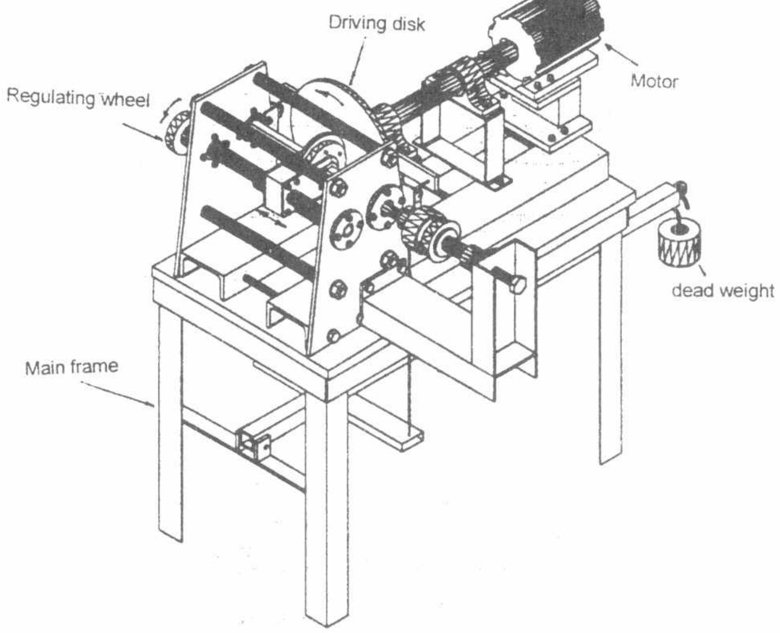

Fig. 3. Global view of the test rig

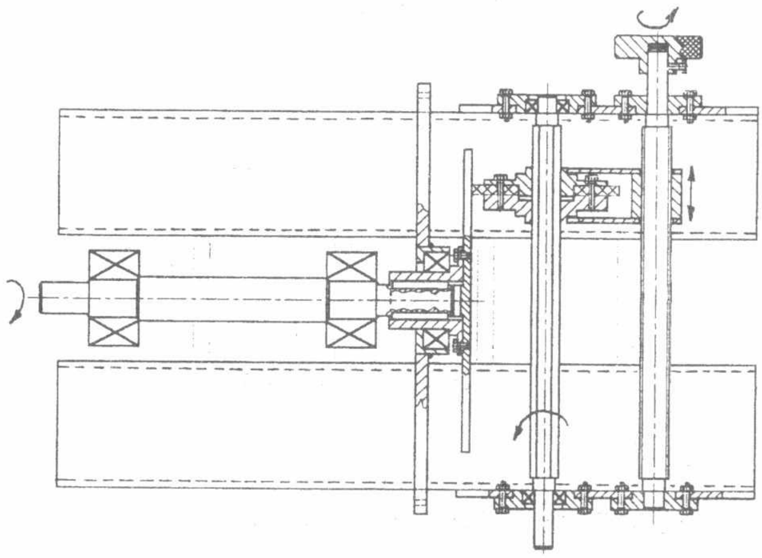

Fig.4. Sectional plan of the test rig

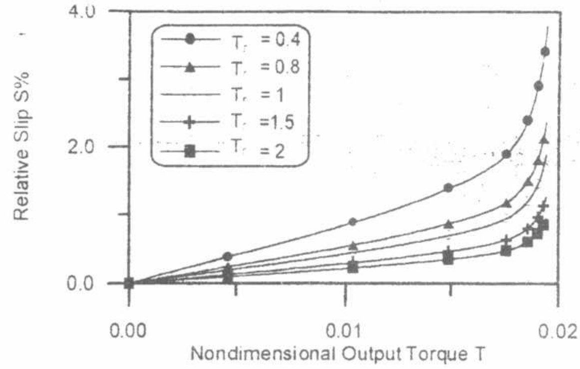

Fig.5. Variation of the relative slip with output torque of an elliptical contact drive at different transmission ratios

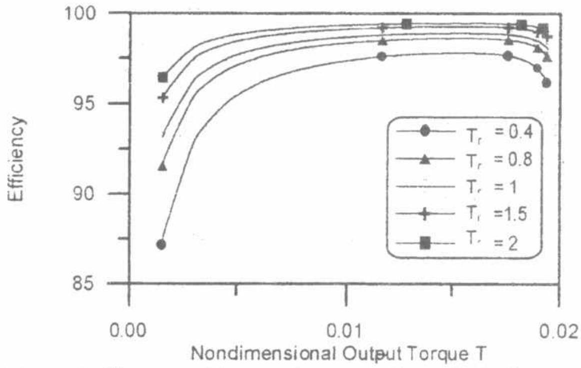

Fig.6. Variation of efficiency with output torque of an elliptical contact drive at different transmission ratios

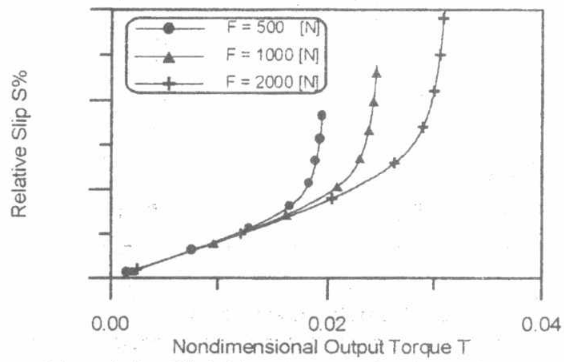

Fig.7. Variation of the relative slip with output torque of an elliptical contact drive at different normal clamping forces

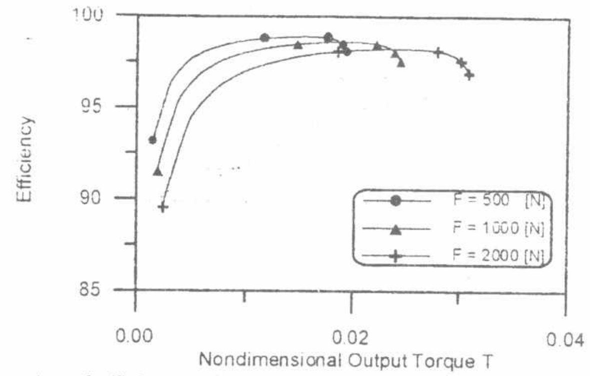

Fig.8. Variation of efficiency with output torque of an elliptical contact drive at different normal clamping forces

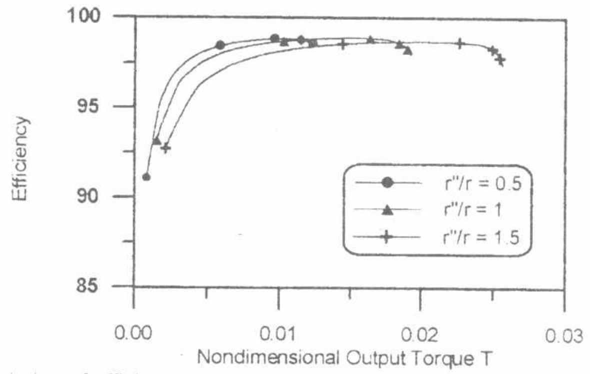

Fig.9. Variation of efficiency with output torque of an elliptical contact drive at different radii ratios

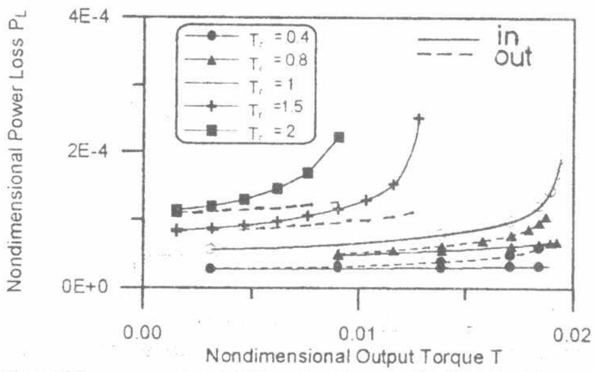

Fig.10. Variation of the power loss with output torque for the double contact drive at different transmission ratios

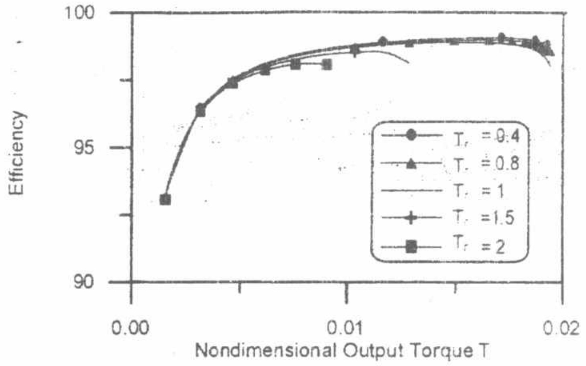

Fig. 11. Variation of efficiency with output torque for the double contact drive at different transmission ratios

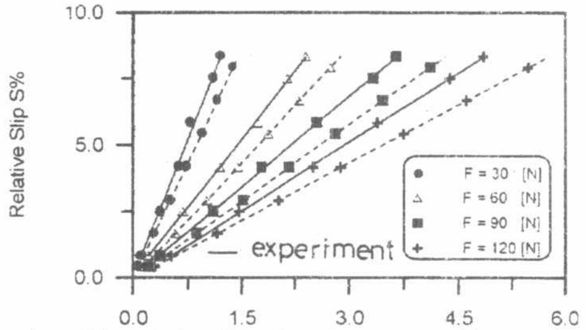

Fig. 12. Variation of the relative slip with output torque of the test rig at different normal clamping forces and $T_{ro} = 2$

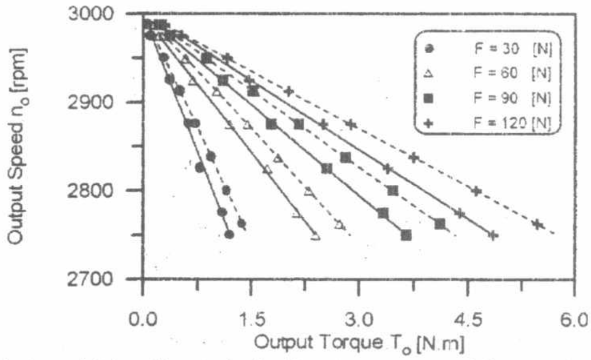

Fig. 13. Variation of the output speed with output torque of the test rig at different normal clamping forces and $T_{ro} = 2$

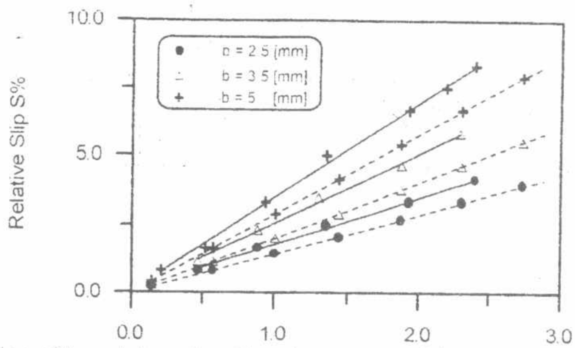

Fig.14. Variation of the relative slip with output torque of the test rig at different width of the driven element and T_{ro} = 2

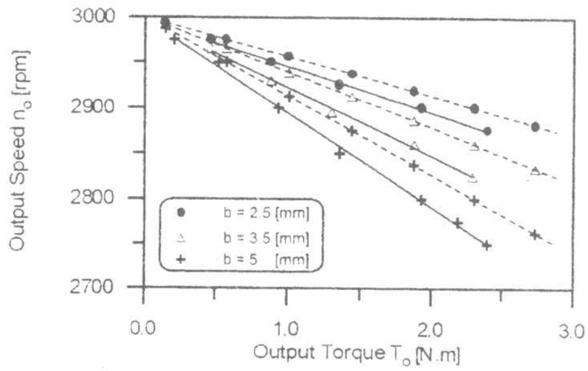

Fig.15. Variation of the output speed with output torque of the test rig at different width of the driven element and T_{ro} = 2

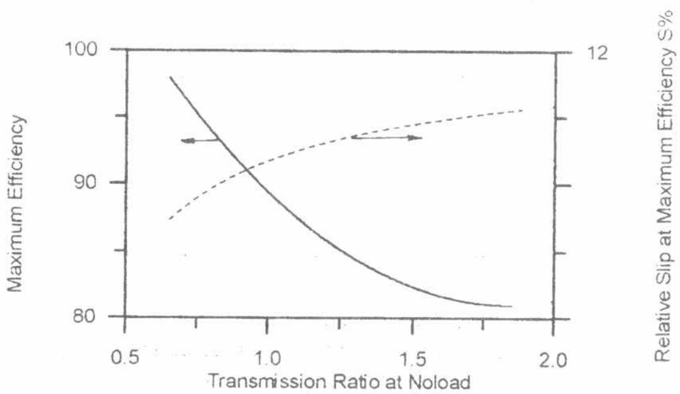

Fig.16. Variation of the maximum efficiency and relative slip of the test rig with the transmission ratios